Check for updates

Neurexophilin 1 suppresses the proliferation of hematopoietic progenitor cells

John Kinzfogl,[1] Giao Hangoc,[1] and Hal E. Broxmeyer[1]

[1]Department of Microbiology and Immunology, Indiana University School of Medicine, Indianapolis, IN

Neurexin I α (NRXN1α) and Dystroglycan (DAG1) are membrane receptors which serve as mutual ligands in the neuronal system. Neurexophilins (NXPHs) bind NRXN1α. NRXN1α was expressed in primitive populations in human CB (huCB) and murine BM (muBM). DAG1 is ubiquitously expressed in hematopoietic tissue; however, osteoblasts appear to be sites of very high expression within muBM. High concentrations of NXPH were found in huCB plasma and murine lineage-positive splenocytes. We evaluated effects of these molecules on huCB and muBM hematopoietic progenitor cells (HPCs) and HSCs. At both a single and population cell level in vitro, we found that NXPH1 was a potent inhibitor of HPC proliferation acting through NRXN1α an effect down-modulated by DAG1. Injection of recombinant NXPH1 in vivo resulted in myelo- and lymphosuppression in the BM, with absolute numbers and cycling status of functional and phenotypically defined HPCs dose- and time-dependently decreased. Competitive HSC transplantations showed no change in the long-term repopulating activity of HSCs from mice exposed to recombinant NXPH1. These results demonstrate the presence and function of a regulated signaling axis in hematopoiesis centered on NRXN1α and its modulation by DAG1 and NXPH1. (*Blood*. 2011;118(3):565-575)

Introduction

Parallels exist between neuropoiesis and hematopoiesis; advances in one field have complemented discoveries in the other.[1,2] Dystroglycan (DAG1) and Neurexin I α (NRXN1α) are membrane proteins that act as receptors or ligands for each other.[3] Failure in mesoderm formation of DAG1 knockout (−/−) mice,[4] suggested to us that the DAG1-NRXN1α signaling axis and its components may play a role in hematopoiesis.

Dystroglycan is a ubiquitously expressed transmembrane glycoprotein encoded by a single gene, *dag1*, whose product is cleaved into a larger 120- to 190-kDa α subunit noncovalently bound to a smaller 43-kDa transmembrane β subunit. DAG1 is the central component of the dystrophin-associated glycoprotein complex and serves as an interface between the cytoskeleton and extracellular matrix. As such, DAG1 is a receptor for multiple extracellular matrix proteins such as Agrin, Laminin, Perlecan, and others.[4] DAG1 can also bind NRXN1α, which is most commonly observed in the brain where normal components of the extracellular matrix are absent.[3] Within the cell, β-DAG1 function is normally associated with dystrophins and syntrophins,[4] though it has also been associated with FYN, C-src tyrosine kinase, Src, NCK1, SHC1, Caveolin-3,[3] and Grb2.[5]

In addition to its role in muscle and brain tissue, DAG1 also plays a role in the hematopoietic system. Blocking DAG1 in the thymus prevents T cells from undergoing positive selection.[6] DAG1 is also highly expressed protein on the surface of cells thought to form the osteoblastic niche for HSCs.[7] In addition, DAG1 knockout mice fail to develop a mesoderm, the embryonic tissue from which hematopoietic cells arise.[4]

The Neurexins are a conserved family of 3 proteins, each with 2 isoforms and numerous splice variants for each isoform.[8] Data from knockout animals suggest that the NRXNs are able to functionally complement each other,[9] though only NRXN1 appears to be expressed in the hematopoietic system.[10] NRXNs are single transmembrane proteins with a small internal PDZ domain and a large extracellular portion whose structure is determined by the isoform. The PDZ domain binds Lin2, a ubiquitously expressed scaffolding protein of the membrane-associated guanylate kinase (MAGUK) family. As a member of the MAGUK family, Lin2 has many binding partners, which obfuscates downstream signaling.[11,12] The larger α-isoform ranges in size from 160-220 kDa and features 6 Laminin, Neurexin, sex hormone–binding protein domain, also known as a Laminin G domain (LNS) repeats as well as an epidermal growth factor (EGF)–like sequence.[13] The shorter β-isoform ranges from 55-95 kDa and lacks the EGF-like sequence and several, though not all, LNS repeats.[3] In both isoforms, splice variants affect the extracellular domain and tend to alter the LNS domains.[14]

In the neuronal system, the primary role of the NRXNs appears to be in directing synapse development, which manifests itself through involvement in calcium signaling, synaptogenesis, and heterogeneous cell-to-cell adhesion—all mediated by a variety of ligands.[9] Because of this, NRXN1α sits at the center of a complex and tightly regulated system. Although NRXN1α possesses 6 LNS domains, most ligands bind either the second or the sixth LNS.[13] The sixth LNS domain is shared with the β-isoform and is primarily involved in GABAergic synapse development. The endogenous activity of the second LNS domain is less well understood, though it is known that DAG1 and the Neurexophilin (NXPH) family are its binding partners.[13]

Because the NXPHs bind the same LNS domain as DAG1,[15] we were also interested in its potential hematopoietic role. The function of NXPH is poorly understood; however, data suggest that

Submitted December 14, 2010; accepted May 13, 2011. Prepublished online as *Blood* First Edition paper, May 31, 2011; DOI 10.1182/blood-2010-12-325381.

The publication costs of this article were defrayed in part by page charge payment. Therefore, and solely to indicate this fact, this article is hereby marked "advertisement" in accordance with 18 USC section 1734.

© 2011 by The American Society of Hematology

Downloaded from http://ashpublications.net/blood/article-pdf/118/3/565/1346345/zh802911000565.pdf by guest on 09 June 2024

they inhibit NRXN-mediated signaling within the neuronal system.[15,16] Furthermore, NXPH occupies the same binding site as DAG1 and binds with a higher affinity,[8] suggesting an antagonistic relationship. In higher mammals, 4 members of the family were identified using sequence homology[17]; of these, NXPH1-3 bind NRXN1α and can complement each other in knockout animals.[8,13,15] NXPH1-3 are small 29 kDa, secreted, neuropeptide-like proteins found in a variety of tissues. In mice, NXPH1 is located primarily in the spleen, NXPH2 is found in the kidney, and NXPH2 and NXPH3 are secreted by a small subset of inhibitory neurons in the brain.[11,17,18] Furthermore, microarray data has implicated high NXPH2 expression in macrophages during immune system exhaustion[19] and many members of the family as a prognostic factor in cancers with a negative prognosis.[20-23] Given its inhibitory role in a neuronal context as well as its presence in immunosuppressive conditions, we hypothesized that NXPH plays an inhibitory role in hematopoiesis.

Methods

Abs and reagents

For flow cytometry, anti–mouse (mu) Abs against c-Kit, Sca-1, FcγR III/II, IL-7Rα, lineage cocktail (CD3, CD14, CD16, CD19, CD20, and CD56), and isotype control Abs were from BD Biosciences. Anti–mu CD34 Ab was from eBioscience and anti–mu sca-1 and lineage cocktail were purchased from BioLegend. Anti–human (hu) CD34, and CD38 were from Biolegend and Miltenyi Biotec; an anti–hu lineage cocktail was from BD Biosciences. In human tissues, DAG1 was analyzed using IIH6 Ab (Santa Cruz Biotechnology) and a PE-conjugated anti–mouse IgM (Santa Cruz Biotechnology); NRXN1α was analyzed using N-16 Ab (Santa Cruz Biotechnology) and APC-conjugated anti–goat IgG Abs (R&D Systems). In murine tissue, DAG1 was analyzed using abcam ab43120 and an APC-conjugated anti–rabbit IgG (Thermo Scientific) for flow cytometry and an HRP-conjugated anti–rabbit IgG Ab (Thermo Scientific) for immunohistochemistry. NRXN1α was analyzed using N-16 Ab (Santa Cruz Biotechnology) and APC-conjugated anti–goat IgG Abs (R&D Systems) for flow cytometry and Synaptic Systems (Goettingen) Ab 175 002 and Thermo Scientific HRP-conjugated anti–rabbit Ab for immunohistochemistry. Before sorting, the $CD34^+$ population of huCB and the lineage-negative population of muBM were enriched via MACS (Miltenyi Biotec).

Abs for Western blots were: anti-NRXN1α mouse mAb (BD Pharmingen), anti-NRXN1α goat polyclonal Ab, anti-NXPH1 goat polyclonal Ab (Santa Cruz Biosystems), and anti–β-actin mu mAb (Sigma-Aldrich). Recombinant rat NXPH1 and NRXN1α were from R&D Systems. All murine recombinant cytokines including SCF, GM-CSF, and IL-3, as well as human recombinant IL-8 were from R&D Systems. Human recombinant cytokines including SCF, GM-CSF, IL-3, thrombopoietin (TPO), and fms-like tyrosine kinase receptor-3 ligand (Flt3L) were from BioVision. Recombinant human erythropoietin (EPO) was from Amgen. FBS was from Hyclone. Growth media including IMDM and RPMI 1640 were from Invitrogen and McCoy 5A was from Sigma-Aldrich. Dulbecco PBS (DPBS) was from Invitrogen, and was only used during in vivo injections; otherwise, PBS from Lonza was used. Pokeweed mitogen mouse spleen cell conditioned medium (PWMSCM) was produced.[24] Propidium iodide (PI) and BrdU were purchased from Sigma-Aldrich.

Mice

C57bl/6 mice were from The Jackson Laboratory. BoyJ mice and C57/BoyJ F1 mice were bred at Indiana University Laboratory Animal Resource Center. Studies were approved by Indiana University Animal Care Committee. In some cases, mice were intravenously injected with either sterile pyrogen-free DPBS or NXPH1, in the presence or absence of BrdU. Some mice were intraperitoneally injected with rapamycin in addition to other compounds listed here. All materials were purchased certified endotoxin free.

Human CB and PB

CB and PB were obtained with institutional review board approval. Low-density (LD) mononuclear CB cells and plasma were isolated by density gradient centrifugation over Ficoll-Plaque Plus (Amersham Pharmacia Biotech). Before sorting, $CD34^+$ cells were enriched via MACs. After enrichment via MACS, cells were sorted via FACS to a final purity of $> 98\%$ $CD34^+$. RBC lysis buffer was used to remove erythrocytes.

Analysis of surface markers, sorting, and plating

Freshly harvested murine BM was washed, resuspended in PBS + 2mM EDTA + 0.5% BSA, incubated for 10 minutes at room temperature with Fc-block, and incubated for 1 hour at 4°C with the recommended volume of anti–murine Abs: lineage cocktail conjugated to APC, c-kit conjugated to PE/Cy5, Sca1 conjugated to PE, and CD34 conjugated to FITC. After incubation, cells were washed and resuspended in PBS and kept at 4°C until sorting by FACSAria (BD Immunocytometry Systems). Freshly harvested and cytokine expanded human $CD34^+$ cells were stained with anti-hu Abs: CD34 conjugated to either FITC or PE. Sorted cells were collected in a solution of PBS + 2mM EDTA + 0.5% BSA, washed, and resuspended in IMDM. For single-cell plating, single $CD34^+$ cells were directly sorted into one well of a 96-well microtiter plate containing 100 μL of methylcellulose (1%) culture medium. Cultures contained IMDM, 30% FBS, and one or more cytokines. At least 216 wells were used per point per experiment.

Phenotypic analysis

Stem and progenitor populations were assessed: long-term repopulating HSCs (LTR-HSC; lineage$^-$sca-1$^+$c-kit$^+$IL-7Rα$^-$CD34$^-$), short-term repopulating HSCs (STR-HSC; lineage$^-$sca-1$^+$c-kit$^+$IL-7Rα$^-$CD34$^+$), common lymphoid progenitor (CLP; lineage$^-$ Sca1$^+$c-kit$^+$IL-7Rα$^+$), megakaryocyte/erythroid progenitor (MEP; lineage$^-$Sca1$^-$c-kit$^+$CD34$^-$FcγR$^{-/lo}$), common myeloid progenitor (CMP; Lin$^-$Sca1$^-$c-kit$^+$CD34$^+$FcγR$^{-/lo}$), and granulocyte/macrophage progenitor (GMP; Lin$^-$Sca1$^-$c-kit$^+$CD34$^+$FcγR$^{+/hi}$). Data were collected from samples using a LSR II (BD Biosciences) instrument and BD FACSDiva software (BD Biosciences) and analyzed using WinList software (Verity Software House).[25]

HPC colony assay

HPC assays were performed as described.[26] Murine BM and spleen cells were plated, respectively, at 5×10^4 and 5×10^5 cells/mL. Cultured in triplicate, cells were incubated in humidified atmosphere, 5% CO_2 and lowered (5%) O_2 at 37°C for 7 days. LD huCB cells were plated between 1 and 5×10^4 cells/mL, while $CD34^+$ enriched cells were plated between 1 and 5×10^2 cells/mL. Human cells were cultured under the same conditions as the murine cells, but with human cytokines, and colonies counted after 14 days of incubation. The following cytokine concentrations were used in vitro: hu and mu GM-CSF or IL-3 (10 ng/mL); hu EPO (1 U/mL); hu and mu SCF (50 ng/mL); PWMSCM (5% vol/vol; a source of many growth factors, including GM-CSF and IL-3). Colonies of CFU-GM, and where appropriate, burst forming unit-erythroid (BFU-E), colony forming unit-granulocyte, erythroid, macrophage, megakaryocte (CFU-GEMM), and total colonies were scored. Absolute numbers of HPCs per femur were calculated. A high specific activity tritiated thymidine kill assay estimated cycling status of HPC (= percent of HPC in S phase).[24,26] To address the issue of DAG1 presence on hu and mu hematopoietic cells, cells were treated for 1 hour using well described IIH6 blocking Ab[6] and then plated.

Western blotting and ELISA

For protein expression, LD muBM and huCB cells were cultured overnight in 5% CO_2 and 5% O_2 at 37°C with growth factors. Cells were washed with ice-cold PBS, lysed, and lysate centrifuged at 14 000*g* for 30 minutes at 4°C. Protein was quantified using bicinchonic acid protein assay reagent (Pierce) and samples adjusted to equal protein concentrations. Total cell

Downloaded from http://ashpublications.net/blood/article-pdf/118/3/565/1346345/zh802911000565.pdf by guest on 09 June 2024

Ai

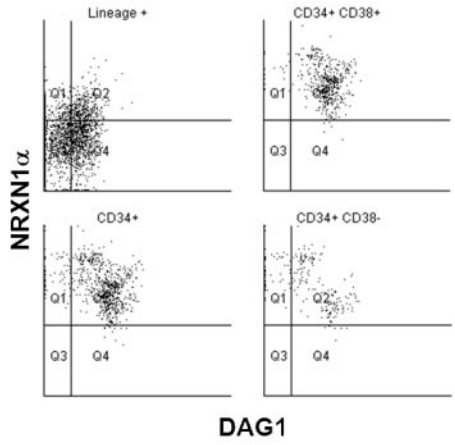

Aii

Cell Type	Percent Cells Expressing: DAG1	NRXN1α	DAG1+ NRXN1α
Lineage+	28.5±6.1	33.8±12.0	21.3±7.1
CD34+	95.4±5.1	95.3±4.4	90.9±8.1
CD34+ CD38+	95.2±4.8	93.6±5.2	90.5±6.8
CD34+ CD38-	93.7±8.7	85.8±16.1	81.8±17.5

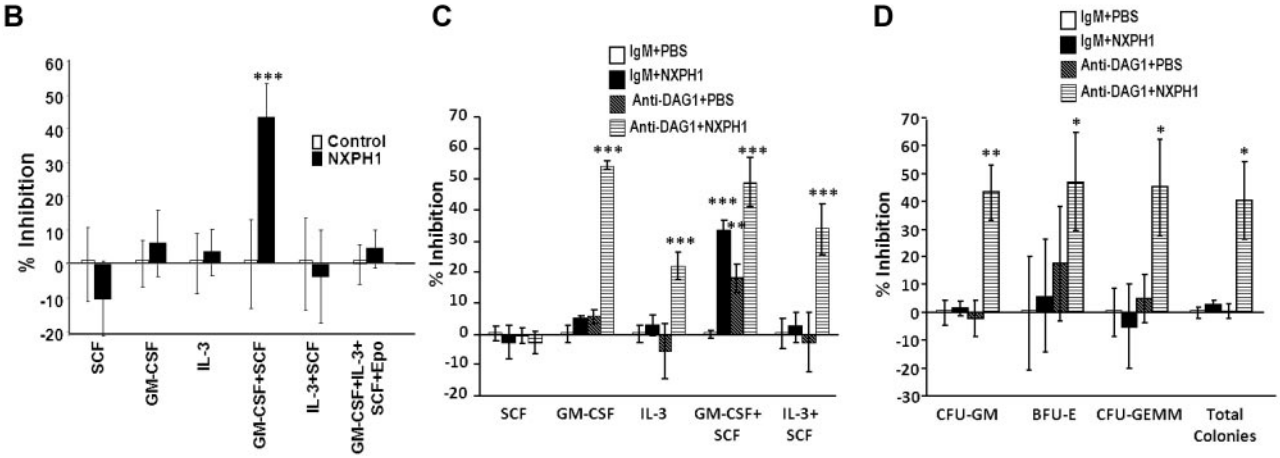

Figure 1. Expression and function of DAG1, NRXN1α, and NXPH in huCB. (Ai) Representative FACS plot of the expression of NRXN1α and DAG1 in huCB populations (For at least 3 independent experiments). (Aii) Chart displaying percentages of huCB populations expressing NRXN1α and DAG1 (combined data from at least 3 independent experiments; mean ± SD). (B) Percent recombinant NXPH1-mediated inhibition of total colony formation in primary huCB cells plated as a population under a variety of factor-stimulated growth conditions (3 combined independent experiments, each done in triplicate; percent inhibition is calculated from the control defined as zero percent inhibition; mean ± SD). (C) Percent recombinant NXPH1-mediated inhibition of CFU-GM colonies produced by huCB-derived HPCs stimulated by specific growth factors, alone or in combination, in the presence and absence of anti-DAG1 blocking Ab when plated in population (combined data from 3 independent experiments performed in triplicate; percent inhibition is calculated from the control defined as zero percent inhibition; mean ± SD). (D) Percent recombinant NXPH1-mediated inhibition of CFU-GM, BFU-E, and CFU-GEMM colonies produced by huCB-derived HPCs stimulated by GM-CSF, IL-3, SCF, and Epo, in the presence and absence of anti-DAG1 blocking Ab when plated in population (combined data from 3 independent experiments performed in triplicate; percent inhibition is calculated from the control defined as zero percent inhibition; mean ± SD). *$P < .05$, **$P < .005$, ***$P < .0005$.

lysates were resolved in 4%-20% gradient SDS-PAGE gels (Invitrogen) and transferred to Hybond membrane (Millipore). Filters were blocked using 5% BSA in TBST for 1 hour and incubated overnight with Abs. Membranes were washed with TBST and incubated with secondary Abs conjugated to HRP, and Ab binding was detected by ECL reaction (GE). ELISA (reagents from BD Pharmingen or R&D Systems) was as described[27] to measure NXPH in muBM, hu and mu PB plasma, and huCB plasma. Polyclonal Ab against full-length recombinant rat NXPH1 (R&D Systems) was used; this Ab likely has little resolution between NXPH1 and other NXPH-family members.

Cell-cycle analysis

Cycling of phenotyped HSCs and HPCs was assayed via PI and BrdU uptake.[28] C57Bl/6 mice were injected intravenously with either carrier (DPBS) plus 1 mg of BrdU or 5 μg of NXPH1 plus 1 mg of BrdU. BrdU (0.8 mg/mL) was also added to drinking water at the time of injection. Twenty-four hours postinjection, BM cells were harvested, washed, and stained for sorting via FACS. After sorting, cells were washed and resuspended in a small volume of ice-cold FBS. Cells were then gently vortexed while ice-cold fixative (95% EtOH and 5% acetic acid) was added to solution. Cells were fixed for 2 hours at 4°C under fluorescent light. Fixed cells were washed and resuspended in PBS and RNase. After RNase digest, DNA was denatured by resuspension in 2N HCL plus Triton X-100. After 30 minutes, cells were pelleted and washed with 0.1M $Na_2B_4O_7$ to neutralize remaining acid. Fixed cells were washed 3 times and resuspended in PBS + 1% Tween + 2% BSA and probed with FITC conjugated anti-BrdU Abs and stained with PI, and analyzed via flow cytometry.

PB analysis

At 24 or 48 hours after intravenous injection of NXPH1, PB was collected by cardiac puncture, and cells analyzed via Hemavet (Drew Scientific Inc).

Competitive repopulation assay

This was performed as described.[29] Briefly, 5×10^5 unsorted BM cells from C57/Bl6 mice (CD45.2) treated 24 hours earlier with either 5 μg of NXPH1 or carrier (DPBS) were mixed with 5×10^5 BoyJ (CD45.1) BM cells and injected by tail vein into C56/Bl6:BoyJ F1 double-positive recipients (CD45.1:CD45.2) which had been total body irradiated with 9.5 Gy. After 7 months, BM was analyzed by flow cytometry using fluorescent-conjugated anti-CD45.1 and CD45.2 Abs and lineage-specific markers (BD Biosciences). After 7 months, 5 secondary recipients per treatment group were transfused with pooled BM from at least 4 members of the corresponding primary transplant group. Four months after the

Downloaded from http://ashpublications.net/blood/article-pdf/118/3/565/1346345/zh802911000565.pdf by guest on 09 June 2024

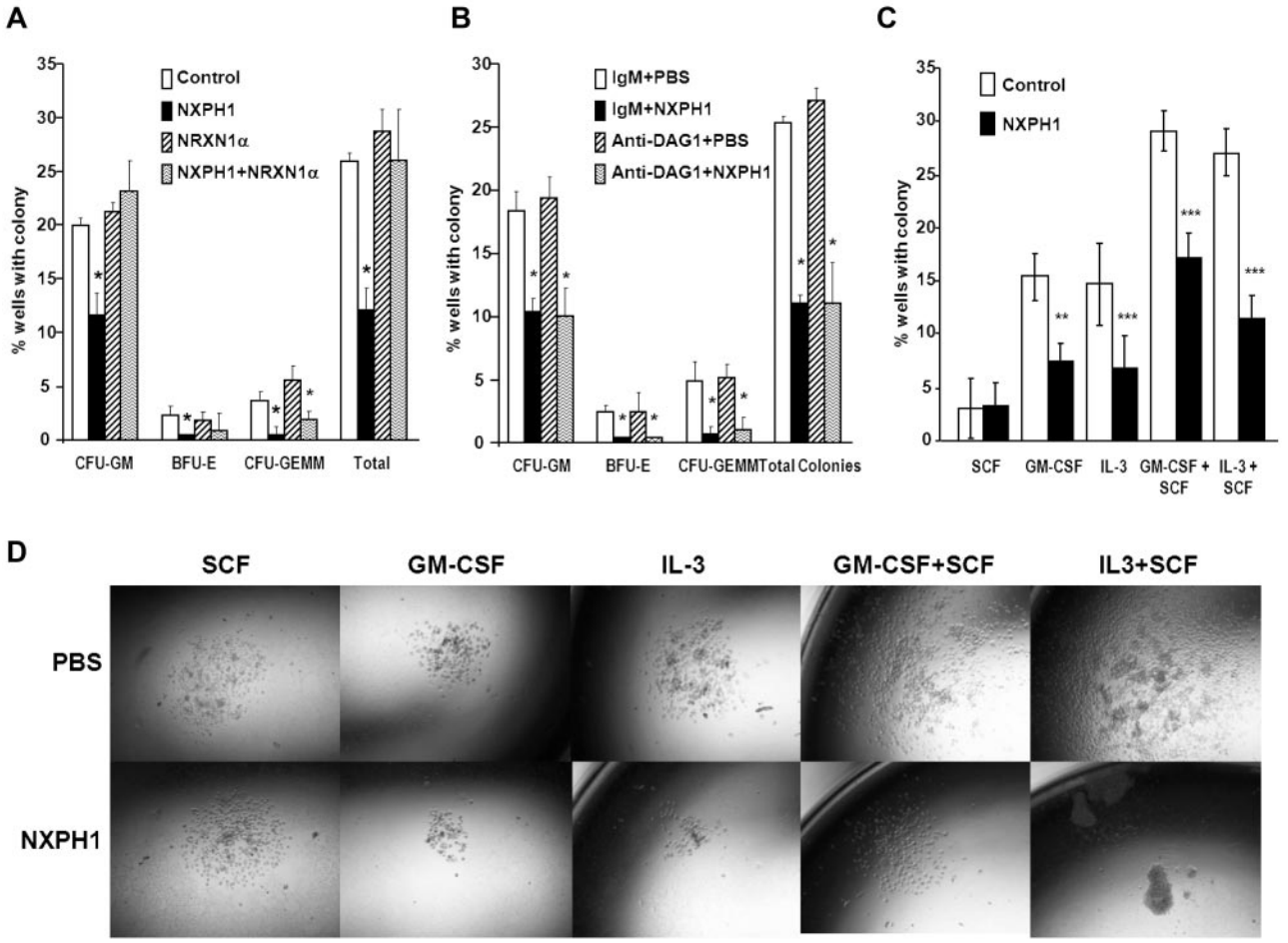

Figure 2. Recombinant NXPH1 directly inhibits colony forming ability and size of primary huCB HPCs. (A) Percent of wells containing individually plated huCB CD34$^+$ cells producing CFU-GM, BFU-E, and CFU-GEMM colonies in the presence of recombinant NXPH1, and/or NRXN1α (252 wells were evaluated for each point; mean ± SD). (B) Percent of wells containing individually plated huCB CD34$^+$ cells producing CFU-GM, BFU-E, and CFU-GEMM colonies in the presence of recombinant NXPH1 and/or anti-DAG1 blocking Ab (252 wells were evaluated for each point; mean ± SD). (C) Percent of wells containing individually plated huCB CD34$^+$ cells grown under a variety of conditions in the presence and absence of recombinant NXPH1-producing CFU-GM colonies (> 500 wells were evaluated for each point; mean ± SD). (D) Size of CFU-GM colonies produced by individually plated huCB CD34$^+$ cells grown under a variety of conditions in the presence and absence of recombinant NXPH1 (representative colonies were selected for display). Microphotographs were taken on a Nikon Labophot with a PLAN objective ×10 (NA 0.3) at room temperature. Images were captured using a 5-mega pixel CCD Nikon DS-Fi1 digital camera in conjunction with NIS-Elements D2.30, Sp1 (Build 325). *$P < .05$, **$P < .005$, ***$P < .0005$.

secondary transplantation, BM was harvested and analyzed for percent chimerism.

Immunohistochemistry

Mouse femurs were dissected and demineralized in a solution of 10% EDTA and 4% phosphate-buffered formalin and then infiltrated with paraffin and sectioned. Detection of DAG1 and NRXN1α expression on paraffin-embedded tibiae from 8- to 16-week-old mice was performed as previously described.[30] Briefly, sections were deparaffinized, treated with 3% H_2O_2 to inhibit endogenous peroxidase activity, blocked with goat serum, and then incubated with either a 1:500 dilution of rabbit polyclonal anti–mouse α-DAG1 Ab or rabbit polyclonal anti–mouse NRXN1α Ab. Sections were then incubated with goat anti–rabbit HRP–conjugated secondary Ab. Color was developed with a diaminobenzidine substrate chromogen system and counterstained with methyl green dye. Nonimmune IgGs were used as negative controls.

Statistical analysis

The Student unpaired 2-tailed *t* test was used (except for the HPC colony assay where single CD34$^+$ cells were plated per well, when the Fisher exact test was used). In experiments involving multiple variables, ANOVA was used between groups to control for false positives. Level of significance is indicated by *P* value. Nonlinear regression analysis was used to generate trend lines. Goodness of fit is indicated by R^2 value.

Results

Expression of DAG1, NRXN1α, and NXPH in huCB

We began our investigation in huCB, as DAG1 has been previously shown to be expressed on a high percentage of CD34$^+$ cells.[31] We found DAG1 and NRXN1α present on nearly all CD34$^+$ cells. Intriguingly, the more primitive CD34$^+$CD38$^-$ population can be further subdivided into 2 distinct populations based on DAG1 and NRXN1α expression (Figure 1Ai-ii); however, these populations do not appear to differ in their proliferation in vitro, nor in their expression of molecules thought to be important to stem cell function such as c-kit, Thy1, CD150, CXCL12 and E-cadherin. Percentage of cells expressing DAG1 and NRXN1α decreased as cells differentiated: only a third of lineage-positive cells expressed either protein. We could not identify a significant population expressing NXPH via flow cytometry; however, ELISA reveals a high concentration (461.7 ± 59.7 ng/mL) of NXPH in huCB

Downloaded from http://ashpublications.net/blood/article-pdf/118/3/565/1346345/zh802911000565.pdf by guest on 09 June 2024

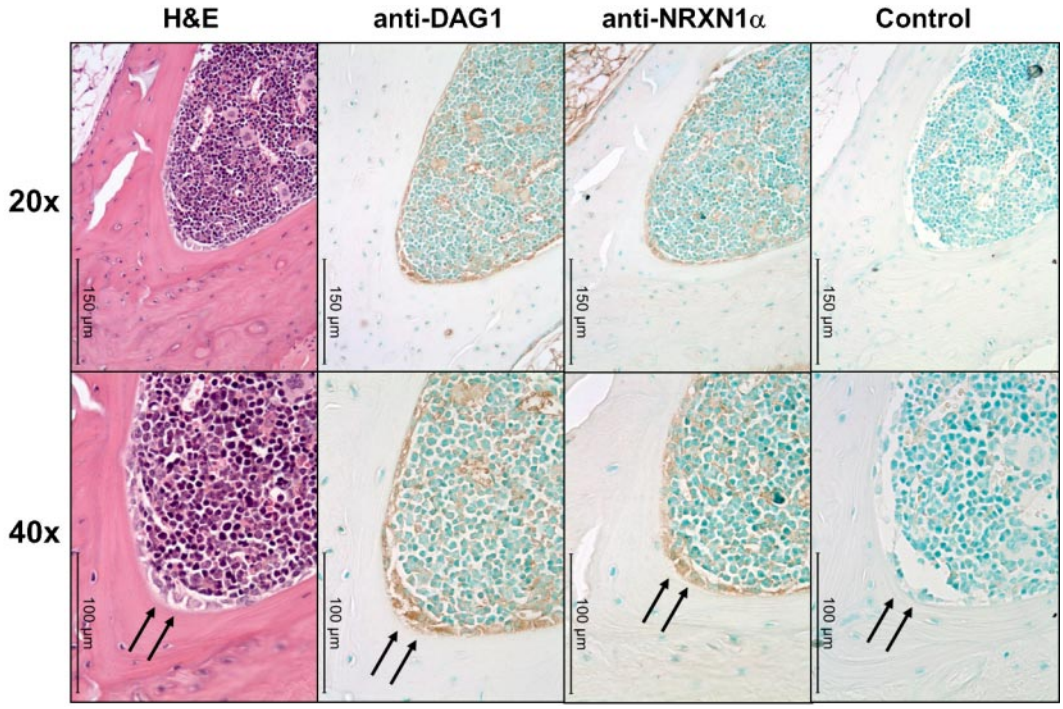

Figure 3. DAG1 and NRXN1α colocalize near osteoblasts in muBM. Low (20×) and higher (40×) power microphotographs of serial sections mounted using Permount mounting medium and stained with H&E or anti–α-DAG1, anti-NRXN1α, rabbit IgG isotype Abs. DAG1 and NRXN1α colocalized to active osteoblasts (marked with an arrow). Immunoreactivity was also observed along the periphery of megakaryocytes and erythrocytes for both DAG1 and NRXN1α. Note the lack of immunoreactivity in osteocytes and stromal cells. Micrographs were taken on a Leica DM3000 microscope with PLAN objective ×20 (NA 0.4) or a PLAN objective ×40 (NA 0.65) at room temperature. Images were captured using Leica Application Suite v3.6.0 from Leica Microsystems.

plasma compared with FBS (8.1 ± 2.1 ng/mL) and adult huPB plasma (5.8 ± 0.8 ng/mL).

Recombinant NXPH1 inhibits colony formation in vitro and is antagonized by endogenous DAG1

Having established the presence of NRXN1α in huCB HPCs, recombinant NXPH1 was used to assay its function. When low-density huCB cells are plated at a concentration of 1×10^4 cells/mL, 200 ng/mL NXPH1 selectively inhibits proliferation stimulated by GM-CSF + SCF (Figure 1B) but not SCF, GM-CSF, IL-3, IL-3 + SCF, and GM-SCF + IL-3 + SCF + Epo. Since DAG1 and NRXN1α are involved in calcium signaling, we hypothesized that DAG1-NRXN1α interaction elicited a prosurvival effect from HPCs, an interaction which was antagonized by recombinant NXPH1. To test for this, huCB cells were preincubated with a DAG1 blocking Ab. Consistent with this hypothesis, cells stimulated with GM-CSF + SCF proliferated less when pre-incubated with the blocking Ab than with the isotype control (Figure 1C). Unexpectedly, when the blocked cells were exposed to recombinant NXPH1, they were inhibited under all growth conditions save SCF alone (Figure 1C-D).

As endogenous DAG1 appeared to be a complicating factor, we sorted individual huCB $CD34^+$ cells to single wells to determine whether suppression was direct on the progenitor cell. Recombinant NXPH1 inhibited proliferation of CFU-GM, BFU-E, and CFU-GEMM progenitors stimulated by GM-SCF + IL-3 + SCF + Epo (Figure 2A). Because recombinant NXPH1 may have been interacting with a previously unrecognized partner, cells were also cultured in the presence of recombinant NRXN1α. Recombinant NRXN1α did not appear to affect proliferation, however, it did decrease the inhibitory effect of recombinant NXPH1 suggesting that recombinant NXPH1 does signal through NRXN1α and exogenous NRXN1α competes with endogenous NRXN1α for binding. To ensure DAG1 had no effect on individual $CD34^+$ cells, $CD34^+$ cells were treated with DAG1 blocking Ab (Figure 2B). Consistent with our hypothesized role for DAG1, no difference was observed between the treated and untreated cells at a single cell level. The effect of recombinant NXPH1 on individually plated $CD34^+$ cells cultured in the presence of SCF, GM-CSF, IL-3, GM-CSF^+SCF, and IL-3 + SCF was also assessed. At a single-cell level, recombinant NXPH1 suppresses colony-forming ability under all conditions save SCF alone (Figure 2C), which is consistent with the huCB cells plated in a population after treatment with anti-DAG1 blocking Ab (Figure 1C). Furthermore, colonies that developed in the presence of recombinant NXPH1 were smaller than those in the controls (Figure 2D). These results suggest that recombinant NXPH1 binds NRXN1α and directly inhibits huCB HPC proliferation. This inhibitory effect is blocked by the presence of DAG1 under all conditions save GM-CSF + SCF, events evaluated below with mouse cells.

Expression of DAG1, NRXN1α and NXPH1 in the murine hematopoietic system

We observed interesting similarities and differences between the huCB and the murine hematopoietic system. The pattern of NRXN1α expression in adult muBM mirrors that found in huCB with a higher percentage of primitive cells expressing NRXN1α while a high percentage of many populations express DAG1, particularly lymphoid progenitors (Table 1). Because NRXN1α expression correlates with a primitive hematopoietic phenotype and DAG1 has been implicated in the hematopoietic niche,[7] we examined the expression pattern of NRXN1α and DAG1 in the BM

Downloaded from http://ashpublications.net/blood/article-pdf/118/3/565/1346345/zh802911000565.pdf by guest on 09 June 2024

Table 1. Expression of NRXN1α and DAG1 in murine BM

	Percentage of cells expressing:	
	NRXN1α	DAG1
LTR-HSC	41.7 ± 3.9	35.9 ± 12.6
STR-HSC	36.7 ± 5.5	61.7 ± 11.8
MEP	21.3 ± 3.4	40.0 ± 9.6
GMP	10.5 ± 1.4	53.3 ± 11.1
CLP	33.6 ± 10.5	95.6 ± 2.1
Lineage$^+$	0.8 ± 0.1	19.4 ± 7.7

LTR-HSC indicates long-term repopulating HSC; STR-HSC, short-term repopulating HSC; MEP, megakaryocyte/erythroid progenitor; GMP, granulocyte/macrophage progenitor; and CLP, common lymphoid progenitor.

using immunohistochemistry. DAG1 is clearly expressed on active osteoblasts within the BM (Figure 3). Cells expressing high levels of NRXN1α in the BM appear to colocalized with cells expressing DAG1, including stromal cells near the osteoblasts. NXPH is not found at concentrations above background in muBM cells and mu peripheral blood plasma; however, previous literature has implicated NXPH in the spleen. Because NXPH is secreted, intracellular staining was used to examine which populations within the spleen express NXPH. A small percent of splenocytes (5.2% ± 0.3%) appear to express NXPH, with the majority of the expression confined to the lineage-positive fraction (7.8% ± 1.0% positive for NXPH). A small percentage of CMPs in the spleen (3.4% ± 0.7%) also contained NXPH.

GM-CSF maintains NRXN1α expression in muBM cells

Similar to huCB, recombinant NXPH1 specifically inhibits proliferation stimulated by GM-CSF + SCF in muBM cells plated in a population (Figure 4A). While the inhibitory effect of blocking DAG1 on GM-CSF + SCF (Figure 1C) demands that other factors are present, we sought to specifically understand the inhibition caused by recombinant NXPH1. To investigate this, we cultured muBM cells under a variety of growth conditions and examined NRXN1α expression via Western blotting (Figure 4Bi-ii). NRXN1α is apparent in freshly isolated cells but when cultured with SCF, IL-3 and IL-3 + SCF, expression level decreases significantly. However, expression of NRXN1α is maintained in cells cultured with either GM-CSF or GM-CSF + SCF. As DAG1 is less expressed on mature cells (Figures 1A, 3, and Table 1), we considered that the ratio of NRXN1α to DAG1 may be altered in favor of available NRXN1α. If true, cells plated in a population would require a higher

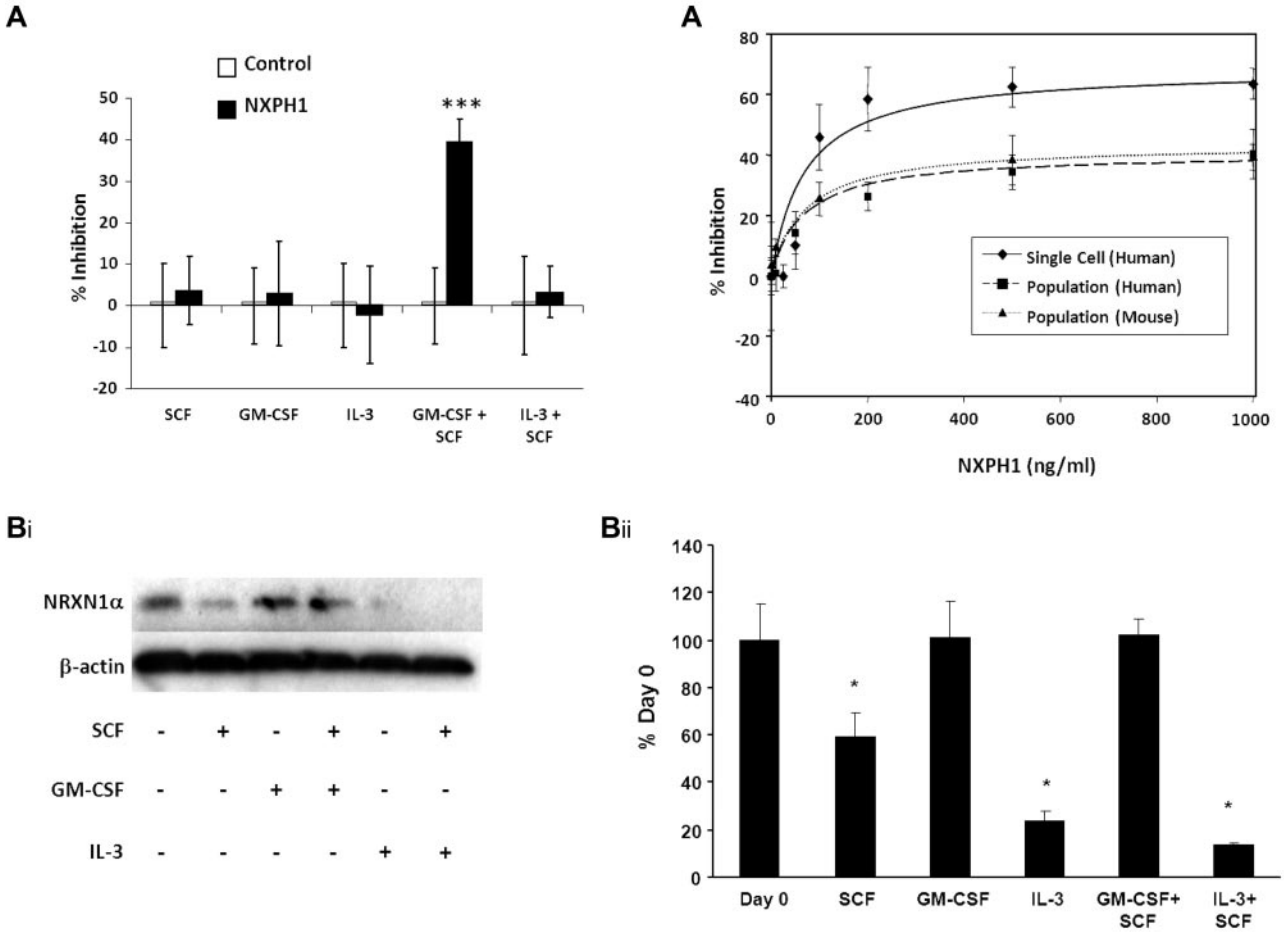

Figure 4. Recombinant NXPH1 inhibits colony forming ability of muBM HPCs. (A) Percent recombinant NXPH1-mediated inhibition of CFU-GM colony formation in primary muBM cells plated as a population under a variety of factor-stimulated growth conditions (3 combined independent experiments, each done in triplicate; mean ± SD). (Bi) Representative Western blot of lysate from primary muBM cells cultured for 24 hours under a variety of conditions. The first lane represents lysate from freshly harvested muBM. β-actin is shown as a loading control. (ii) Densitometric analysis of NRXN1α expression in Western blots. Values were normalized to β-actin and represented as a percent of the day 0 control (4 combined independent experiments; mean ± SD). (C) Calculated dose-response curves modeling the NXPH1-mediated inhibition of CFU-GM colony formation in the presence of GM-CSF + SCF. HPCs were derived from either individually plated huCB CD34$^+$ ($R^2 = 0.95$), huLDCB plated in population (1×10^4cells/mL; $R^2 = 0.99$), or muBM plated in population (5×10^4cells/mL; $R^2 = 0.99$; 288 wells were evaluated for each data point in experiments involving a single plated cell; at least 3 independent experiments performed in triplicate were used for calculating data points involving cells plated in a population; mean ± SD). *$P < .05$, **$P < .005$, ***$P < .0005$.

Downloaded from http://ashpublications.net/blood/article-pdf/118/3/565/1346345/zh802911000565.pdf by guest on 09 June 2024

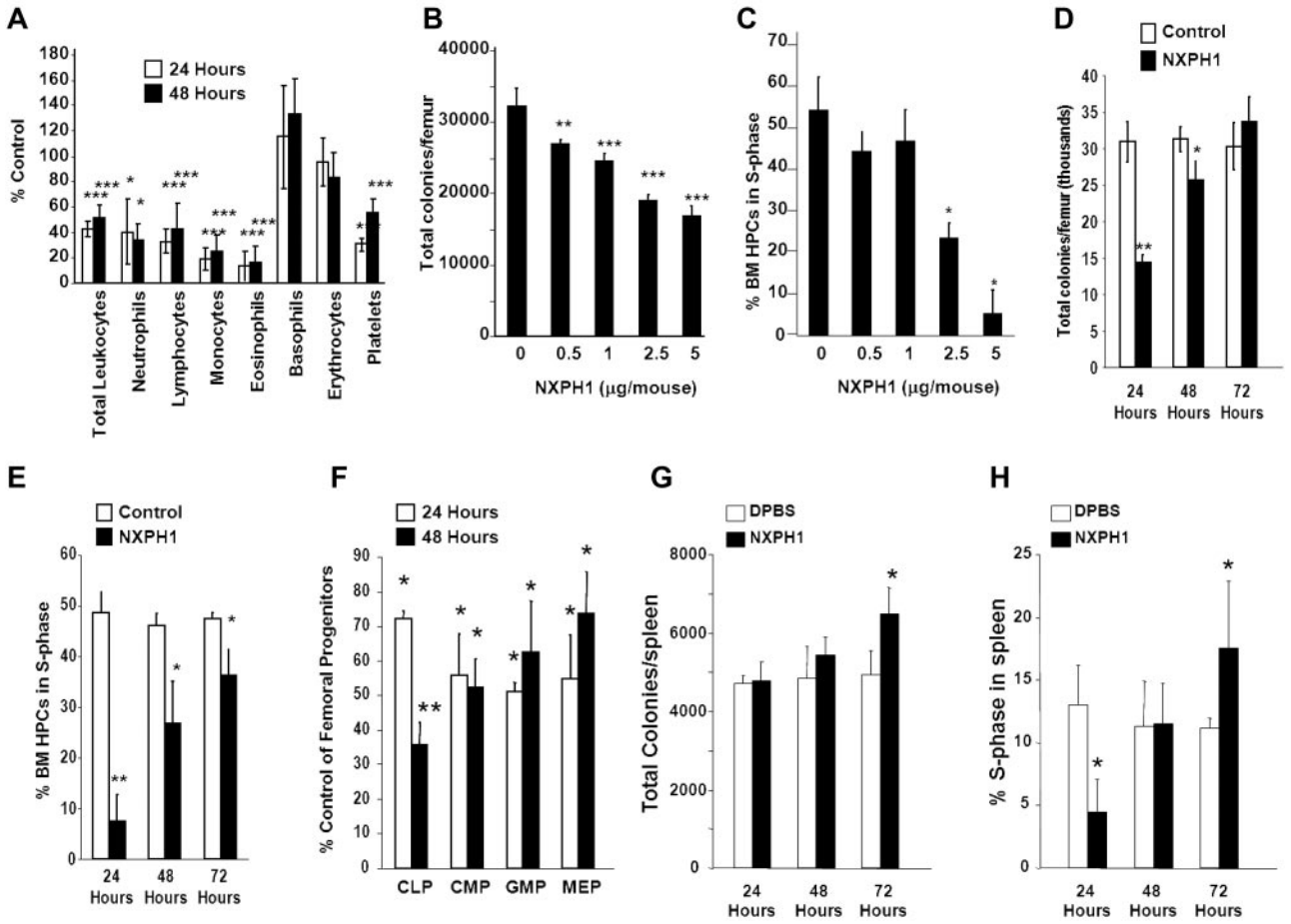

Figure 5. Recombinant NXPH1 decreases absolute numbers and cycling status of HPCs and mature blood cells in vivo. (A) Change in peripheral blood populations after intravenous injection of recombinant NXPH1 expressed as a percentage of control (at least 3 independent experiments performed in triplicate; percent control is calculated from the control defined as 100%; mean ± SD). (B) Absolute colony number of muBM-derived HPCs 24 hours after exposure to varying doses of recombinant NXPH1 (combined data of 3 independent experiments each performed in triplicate; mean ± SD). (C) Cycling status of muBM-derived HPCs 24 hours after exposure to varying doses of recombinant NXPH1 (combined data of 3 independent experiments each performed in triplicate; mean ± SD). (D) Absolute colony number of muBM-derived HPCs 24, 48, and 72 hours after exposure to DPBS carrier or 5 μg/mouse NXPH1 (combined data of 3 independent experiments each performed in triplicate; mean ± SD). (E) Cycling status of muBM-derived HPCs 24, 48, and 72 hours after exposure to DPBS carrier or 5 μg/mouse NXPH1 (combined data of 3 independent experiments each performed in triplicate; mean ± SD). (F) Change in phenotypically defined muBM progenitor populations 24 hours after intravenous exposure to DPBS carrier or 5 μg/mouse NXPH1 expressed as a percent control (combined data of 3 independent experiments each performed in triplicate; mean ± SD). (G) Absolute colony number of spleen-derived HPCs 24, 48, and 72 hours after exposure to DPBS carrier or 5 μg/mouse NXPH1 (combined data of 3 independent experiments each performed in triplicate; mean ± SD). (H) Cycling status of spleen-derived HPCs 24, 48, and 72 hours after exposure to DPBS carrier or 5 μg/mouse NXPH1 (combined data of 3 independent experiments each performed in triplicate; mean ± SD). $^*P < .05$, $^{**}P < .005$, $^{***}P < .0005$.

concentration of recombinant NXPH1 in order for equivalent levels of inhibition to be observed. Human CB and muBM cells respond similarly to recombinant NXPH1 in population with maximal inhibition observed at 500 ng/mL. However, individually plated human $CD34^+$ CB cells reach their maximal inhibition at 200 ng/mL. An examination of the dose-response curves (Figure 4C) reveals that the affinity of NXPH1 to NRXN1α on individually plated $CD34^+$ cells ($IC_{50} = 68.8 \pm 5.9$ ng/mL) is the same as for NXPH1 to NRXN1α on huCB and muBM cells plated in a population ($IC_{50} = 68.7 \pm 1.8$ ng/mL and 71.0 ± 4.8 ng/mL, respectively). However, the efficacy of NXPH1 on individually plated $CD34^+$ cells ($I_{max} = 68.7\% \pm 2.7\%$ inhibition) is much greater than when huCB and muBM cells are plated in a population ($I_{max} = 40.7 \pm 3.3$ and $43.7\% \pm 2.5\%$ inhibition, respectively). From this, we conclude that DAG1 decreases the efficacy of NXPH1 but not its affinity, suggesting that DAG1 is a noncompetitive agonist.

Recombinant NXPH1 exhibits suppressive effects in vivo

Normal C56Bl/6 mice were injected intravenously with endotoxin-free recombinant NXPH1. Twenty-four to 48 hours after injection of recombinant NXPH1, total leukocytes, as well as neutrophils, lymphocytes, monocytes, eosinophils, basophils, and platelets were significantly decreased (Figure 5A). Absolute numbers of HPCs in the BM were decreased in a dose- and time-dependent manner (Figure 5B). At a maximally inhibitory dose (2.5-5 μg NXPH1/mouse), absolute numbers of HPCs were inhibited by 50.8% at 24 hours, effects mirrored by decreases at 24 hours in cycling HPCs, as measured by high specificity activated tritiated thymidine kill assay (Figure 5C). After 48 hours, absolute numbers of HPCs were increased but still significantly inhibited: HPC numbers completely returned to normal levels 72 hours after injection of NXPH1 (Figure 5D), a trend mirrored in the cycling status of BM HPCs (Figure 5E). Consistent with functional data, phenotypically defined BM HPCs were also suppressed by recombinant NXPH1 (Figure 5F) at levels similar to those observed in functional assays. In contrast to the BM, the spleen was less responsive to NXPH1 exposure. At a maximally inhibitory dose (5 μg NXPH1/mouse) absolute numbers of splenic HPCs were unaffected for the first 2 days and increased slightly after the third

Downloaded from http://ashpublications.net/blood/article-pdf/118/3/565/1346345/zh802911000565.pdf by guest on 09 June 2024

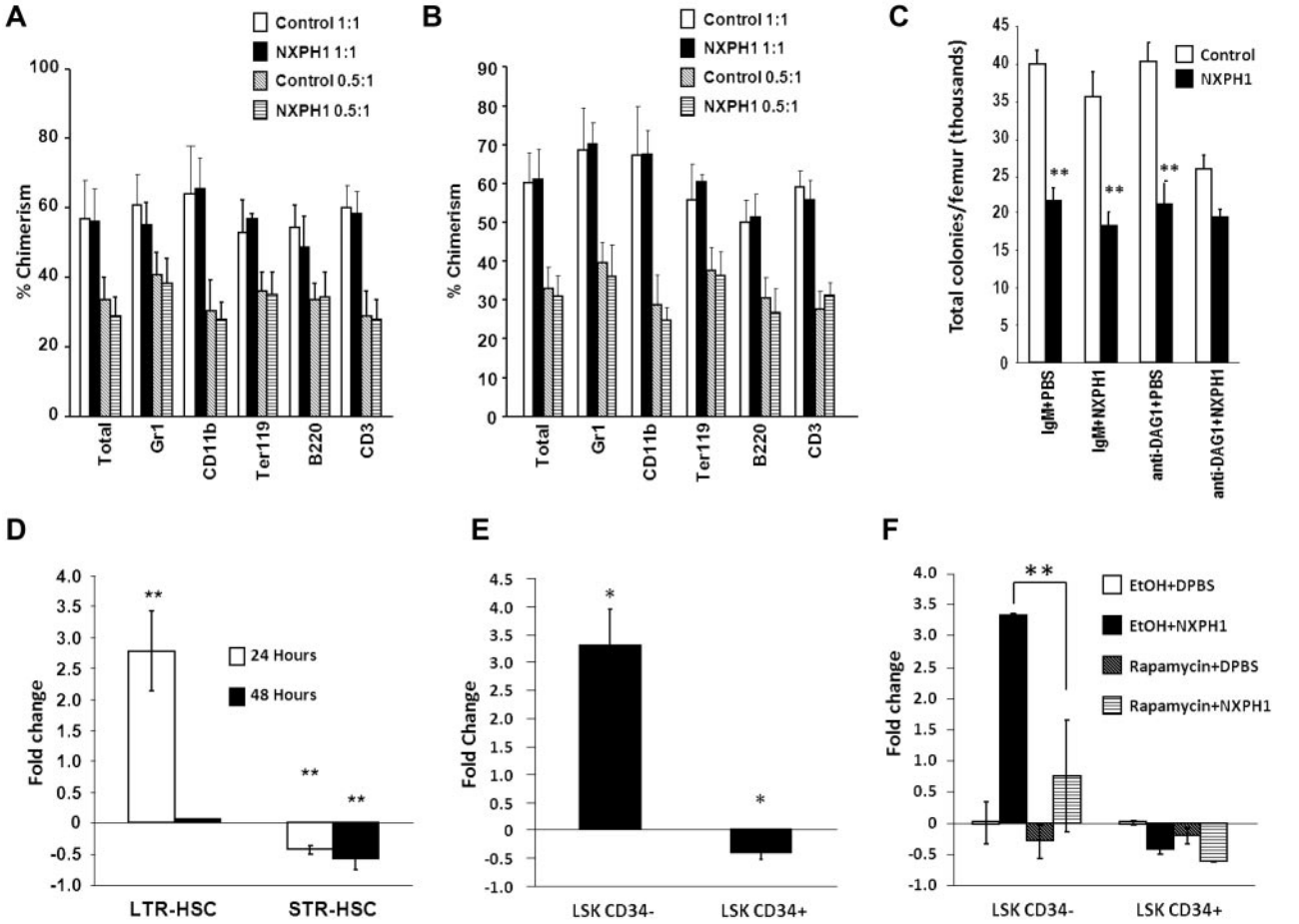

Figure 6. Recombinant NXPH1 does not affect primitive hematopoietic cells in vivo. (A) Percent chimerism of donor cells in total BM, as well as several lineage-restricted populations in primary recipients after 7 months. In the competitive repopulation assay, pooled BM from 3 C57Bl/6 mice per treatment group was combined either 1:1 or 0.5:1 with BoyJ competitor cells 24 hours after treatment of mice with DPBS carrier or 5 μg/mouse recombinant NXPH1 and transplanted into 5 mice per treatment group (mean ± SD). (B) Percent chimerism in total BM, as well as several lineage-restricted populations in secondary recipients derived from either 1:1 or 0.5:1 primary competitive repopulation assay. After 7 months, 5 secondary recipients per treatment group were transfused with pooled BM from at least 4 members of the corresponding primary transplant group. Four months after the secondary transplant, BM was harvested and analyzed for percent chimerism was analyzed (mean ± SD). (C) Effect of in vitro exposure to recombinant NXPH1 on muBM total CFUs derived from mice treated with recombinant NXPH1 in vivo. Mice were intravenously injected with either DPBS carrier or 5 μg of recombinant NXPH1. Twenty-four hours after in vivo exposure, BM was harvested and treated with either mouse IgM or anti-DAG1 blocking Ab in vitro and then plated in SCF, GM-CSF, PWMSCM, and Epo ± 200 ng/mL recombinant NXPH1 (combined data of 3 animals each analyzed in triplicate; mean ± SD). (D) Fold change in vivo of phenotypically defined HSCs 24 and 48 hours after injection of 5 μg/mouse recombinant NXPH1 (combined data from 2 independent experiments performed in triplicate; mean ± SD). (E) Fold change in cycling status of populations heavily enriched for long (LSK CD34$^-$) or short (LSK CD34$^+$) term engrafting HSCs 24 hours after injection of 5 μg/mouse recombinant NXPH1(combined data from 2 independent experiments performed in triplicate; mean ± SD). (F) Fold change in phenotypically defined HSCs 24 hours after 5 μg/mouse intravenous recombinant NXPH1 exposure and 5 mg/mouse intraperitoneal rapamycin injection (combined data from 2 independent experiments performed in triplicate; mean ± SD). *$P < .05$, **$P < .005$, ***$P < .0005$.

day (Figure 5G). The cycling status of splenic HPCs was decreased 24 hours after injection but returned to baseline after 48 hours, and was slightly increased after 72 hours (Figure 5H).

Primitive HSCs are bound to DAG1 in vivo

To determine effects of NXPH on functional HSCs, C57Bl/6 mice (CD45.2$^+$) were intravenously injected with either 5 μg of recombinant NXPH1 or DPBS carrier. BM was collected from these treated mice after 24 hours, and these cells combined at equal cell numbers with untreated competitor BM cells from BoyJ mice (CD45.1$^+$). Lethally irradiated C57/BoyJ F1 mice had their hematopoietic system reconstituted using these cells. After 7 months, no effect on long-term competitive repopulation potential was observed during the primary transplant (Figure 6A). To further characterize the effect of NXPH1 on the LTR-HSC compartment, 2×10^6 total BM cells from the primary recipients were transfused into a second set of lethally irradiated C57/BoyJ F1 mice. After 4 months, the secondary recipients were killed and the percent chimerism in the total BM as well as specific lineage populations was examined (Figure 6B). Consistent with the data from month 6 of the primary transplant, no difference was found between the experimental condition and control. This suggested that NXPH1 does not have an effect on the long-term repopulating potential of primitive HSCs.

We had demonstrated using single-cell culture and DAG1 blocking Abs that DAG1 counteracts the suppressive effects of NXPH1 on HPCs in vitro. As absolute numbers of femoral HPCs are suppressed by in vivo administration of NXPH1 while the long-term repopulating potential of primitive HSCs was unaffected, we hypothesized that only primitive HSCs are bound to DAG1 in vivo. To test this, muBM cells harvested from control and NXPH1-treated mice were treated with DAG1 blocking Ab before in vitro culture in presence of NXPH1. If HPCs were influenced by DAG1 in vivo, HPCs removed from mice exposed to NXPH1 in vivo ought to be further inhibited by anti-DAG1 + NXPH1 in vitro. Conversely, if HPCs are not influenced by DAG1 in vivo, in

Downloaded from http://ashpublications.net/blood/article-pdf/118/3/565/1346345/zh802911000565.pdf by guest on 09 June 2024

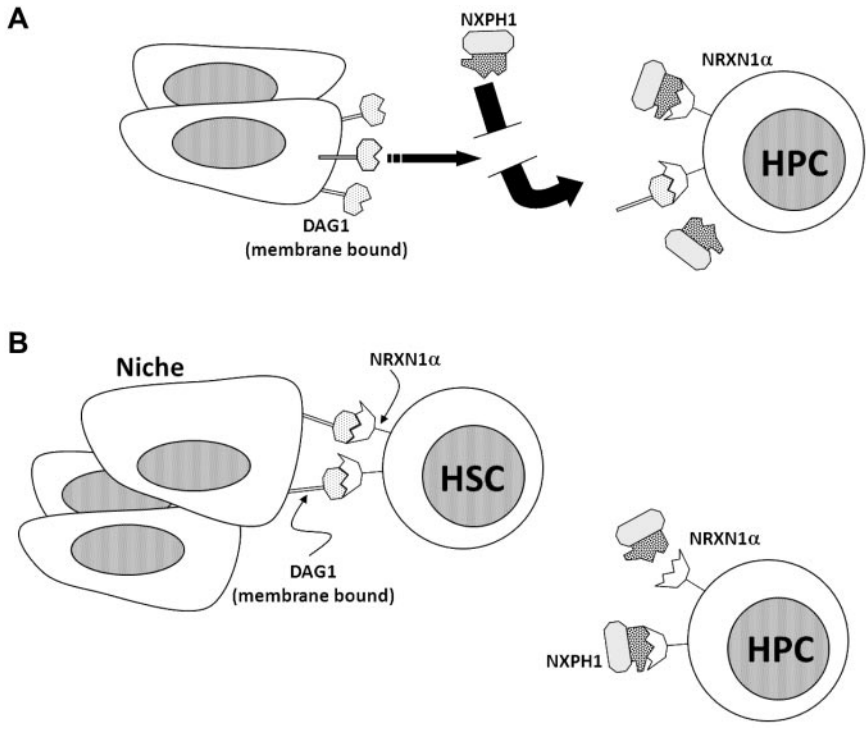

Figure 7. Diagrammatic role of NRXN1α, DAG1, and NXPH1 in the hematopoietic system. (A) NRXN1α, DAG1, and recombinant NXPH1 as they behave in the hematopoietic model in vitro. (B) Hypothetical interaction of NRXN1α, DAG1, and recombinant NXPH1 in vivo.

vitro exposure to anti-DAG1 + NXPH1 ought not be inhibitory, due possibly to either maximal inhibition or receptor down-regulation. We found no further inhibition of HPCs after in vitro exposure to anti-DAG1 + NXPH1, supporting the hypothesis that HPCs are not likely influenced by DAG1 in vivo (Figure 6C).

To determine which populations were affected by NXPH1 in vivo, phenotypically defined BM HSCs/HPCs were examined 24 and 48 hours after mice were injected intravenously with recombinant NXPH1. Consistent with HPC data, STR-HSCs were suppressed at both time points. Cells categorized in the longer-term population of HSCs experienced significant increase in numbers after 24 hours, but had returned to baseline after 48 hours (Figure 6D). To further investigate this, normal C57Bl/6 mice underwent the same injection procedure, but with addition of BrdU. BrdU was coinjected with recombinant NXPH1 and placed in drinking water after mouse exposure to NXPH1. Twenty-four hours after exposure of mice to NXPH1 or control media, BM cells from treated and untreated mice were sorted into: KSL CD34$^-$ (c-kit$^+$, sca1$^+$, lineage$^-$ CD34$^{lo/-}$) and KSL CD34$^+$ cells. Mirroring functional and phenotypic data, KSL CD34$^+$ cells experienced a 38% decrease in percentage of cells in S phase, while KSL CD34$^-$ cells from NXPH1-treated mice had a 3.7-fold increase in cycling cells (Figure 6E). In both conditions, the cells entering S phase appeared to come from cells in G1/G0 as a corresponding decrease in total percentage was observed in these populations suggesting cell-cycle arrest. Because cell-cycle arrest is often associated with apoptosis, we examined extracellular annexin V expression on the phenotypically defined populations in treated and untreated mice; however, no increase in apoptosis was observed in the treated mice (data not shown).

There are 2 possible interpretations for increases in numbers and cycling status of phenotyped LTR-HSCs: either NXPH1 directly induces cycling, or cycling is perhaps induced to reassert homeostasis challenged by inhibitory effects of NXPH1 on HPCs. In the hematopoietic system, the mTOR pathway is involved in stress responses[29] consistent with the second interpretation, so cycling status of both the LTR- and STR-HSCs was examined in mice treated in the same manner as the previous experiment but with intraperitoneal injection of rapamycin or ethanol carrier immediately before NXPH1 intravenous injection. Exposure of mice to rapamycin inhibited increases in cycling of KSL CD34$^-$ cells while leaving KSL CD34$^+$ cells unaffected (Figure 6F). Because our results show that mTOR is at least partially involved in stimulation of LTR-HSCs in response to NXPH1 exposure in vivo, but is not involved in NXPH1-mediated inhibition of STR-HSCs, and because induction of the mTOR pathway in LTR-HSCs has been associated with a homeostatic stress response,[29] we believe that LTR-HSCs are not directly affected by NXPH1 and the observed increase in phenotypically defined HSCs is because of a homeostatic response mediated at least partially through the mTOR pathway.

Discussion

A signaling axis centered on the second LNS domain of NRXN1α is present and functional in the hematopoietic system. Expression of NRXN1α correlates with primitive hematopoietic populations, while DAG1 is heavily expressed on active osteoblasts in the BM and is also present on many hematopoietic cells. The third member of the axis, the NXPH family, is found in huCB plasma and within lineage-positive cells in the mouse spleen. We found that recombinant NXPH1 acts as a potent inhibitor of HPC proliferation in vivo and in vitro; however, this inhibition is allosterically inhibited by the presence of DAG1. We suggest that NXPH directly acts to suppress hematopoiesis, and a role of DAG1 is to occupy NRXN1α, thereby preventing excess inhibition (see model in Figure 7A).

The involvement of the NRXN1α axis in hematopoiesis may prove to be of clinical relevance. Recombinant NXPH1 does not affect the function of primitive HSCs; however, it does inhibit the proliferation of HPCs including those from huCB, unlike inhibitory chemokines.[32] Taken in consideration with high levels of NXPH

Downloaded from http://ashpublications.net/blood/article-pdf/118/3/565/1346345/zh802911000565.pdf by guest on 09 June 2024

found in huCB plasma, we suggest that this may in part explain the long engraftment time observed in patients receiving huCB transplants. The differing responses of these populations to recombinant NXPH1 may also explain the correlation between high levels of NXPH expression and aggressive cancers.[20-23] If cancer stem cells are protected from NXPH in a manner similar to HSCs, secreted NXPH would inhibit hematopoietic cells involved in the immune response while leaving the cancer cells relatively unaffected.

The role of this axis in healthy animals is less clear; however, human disease models may provide insight. Disruption of NRXN1α or proteins directly downstream correlates very strongly with schizophrenia[33] and certain disorders along the autistic spectrum.[34] Both diseases manifest a proinflammatory phenotype coupled with an increase in numbers and cycling of hematopoietic populations including HPCs.[35-40] This mirrors the hematopoietic behavior of mice exposed to recombinant NXPH1, which respond less well to cytokines and experience a decrease in absolute number and cycling status of HPCs. Taken together with the NXPH presence in the spleen and huCB plasma, this may explain the relatively quiescent state of HPCs in these tissues.

Another interesting finding was DAG1 expression in the BM. Although DAG1 appears to be expressed on many cells in the BM, histology reveals that it is most heavily expressed in osteoblasts. The colocalization of DAG1 and NRXN1α in the BM observed together with the physiologic response of hematopoietic cells to recombinant NXPH1 exposure leads us to hypothesize that primitive HSCs are bound to DAG1 in the niche, whereas less primitive HSCs and HPCs tend not to be bound to DAG1 in vivo. This model (diagrammed in Figure 7B) suggests that one role of DAG1 in hematopoiesis may be to "protect" hematopoietic cells from exposure to members of the NXPH family. Furthermore, DAG1 is required for synapse development under many conditions,[6,41] which creates the possibility that the DAG1-NRXN1α interaction may be involved in the development of the hematopoietic niche. Of technical relevance, the similarities between osteocytes and osteoblasts make them difficult to distinguish[30,42]; however, the high DAG1 level of expression observed in osteoblasts provides a convenient marker.

We have demonstrated that 3 previously identified elements of the neuronal system: DAG1, NRXN1α, and NXPH1, and perhaps other members of the NXPH family, are present and functional within the hematopoietic system and form a tightly regulated axis. DAG1 appears to bind NRXN1α, and protect HPCs from NXPH1 binding and subsequent inhibition. In vivo, this protection is observed on phenotypically defined LTR-HSCs, suggesting that the DAG1-NRXN1α axis may play a significant role in the hematopoietic niche. In addition to their scientific value, these results have potential clinical implications. High concentrations of NXPH in huCB may at least partially be involved in delayed time to engraftment for CB transplants, while high NXPH expression, which correlates with a negative prognosis in cancer, may be involved in immune system evasion by cancer. Further studies in these areas are of experimental and clinical interest.

Acknowledgments

The authors thank Keith Condon for his expertise in immunohistochemistry and generous use of reagents.

This work was supported by US Public Health Service Grants NIH R01 HL56416 and NIH R01 HL67384 from the National Institutes of Health (H.E.B.). J.K. was supported sequentially by NIH T32 HL07910 and then DK07519 training grants to H.E.B.

Authorship

Contribution: J.K. performed and designed research, analyzed and interpreted the data, and wrote the manuscript; G.H. performed research and analyzed the data; and H.E.B. analyzed and interpreted the data, supported the research, and fixed the manuscript.

Conflict-of-interest disclosure: The authors declare no competing financial interests.

Correspondence: Hal E. Broxmeyer, PhD, Department of Microbiology and Immunology, Indiana University School of Medicine, 950 W Walnut St, R2-302, Indianapolis, IN 46202-5181; e-mail: hbroxmey@iupui.edu.

References

1. Terskikh AV, Easterday MC, Li L, et al. From hematopoiesis to neuropoiesis: evidence of overlapping genetic programs. *Proc Natl Acad Sci U S A.* 2001;98(14):7934-7939.
2. Mendez-Ferrer S, Lucas D, Battista M, Frenette PS. Haematopoietic stem cell release is regulated by circadian oscillations. *Nature.* 2008; 452(7186):442-447.
3. Sugita S, Saito F, Tang J, et al. A stoichiometric complex of neurexins and dystroglycan in brain. *J. Cell Biol.* 2001;154(2):435-445.
4. Williamson RA, Henry MD, Daniels KJ, et al. Dystroglycan is essential for early embryonic development: disruption of Reichert's membrane in Dag1-null mice. *Hum Mol Genet.* 1997;6(6):831-841.
5. Yang B, Jung D, Motto D, Meyer J, Koretzky G, Campbell KP. SH3 domain-mediated interaction of dystroglycan and Grb2. *J Biol Chem.* 1995; 270(20):11711-11714.
6. Zhang J, Wang Y, Chu Y, et al. Agrin is involved in lymphocytes activation that is mediated by alpha-dystroglycan. *FASEB J.* 2006;20(1):50-58.
7. Hines M, Nielsen L, Cooper-White J. The hematopoietic stem cell niche: what are we trying to replicate? *J Chem Technol Biotechnol.* 2008;83: 421-443.
8. Missler M, Sudhof TC. Neurexophilins form a conserved family of neuropeptide-like glycoproteins. *J Neurosci.* 1998;18(10):3630-3638.
9. Missler M, Zhang W, Rohlmann A, et al. Alpha-neurexins couple Ca2+ channels to synaptic vesicle exocytosis. *Nature.* 2003;423(6943):939-948.
10. Ivanova NB, Dimos JT, Schaniel C, et al. A stem cell molecular signature. *Science.* 2002; 298(5593):601-604.
11. Craig AM, Kang Y. Neurexin-neuroligin signaling in synapse development. *Curr Opin Neurobiol.* 2007;17(1):43-52.
12. Hata Y, Butz S, Sudhof TC. CASK: a novel dlg/PSD95 homolog with an N-terminal calmodulin-dependent protein kinase domain identified by interaction with neurexins. *J Neurosci.* 1996; 16(8):2488-2494.
13. Lise MF, El-Husseini A. The neuroligin and neurexin families: from structure to function at the synapse. *Cell Mol Life Sci.* 2006;63(16):1833-1849.
14. Ushkaryov YA, Hata Y, Ichtchenko K, et al. Conserved domain structure of beta-neurexins. Unusual cleaved signal sequences in receptor-like neuronal cell-surface proteins. *J Biol Chem.* 1994;269(16):11987-11992.
15. Beglopoulos V, Montag-Sallaz M, Rohlmann A, et al. Neurexophilin 3 is highly localized in cortical and cerebellar regions and is functionally important for sensorimotor gating and motor coordination. *Mol Cell Biol.* 2005;25(16):7278-7288.
16. Zhang W, Rohlmann A, Sargsyan V, et al. Extracellular domains of alpha-neurexins participate in regulating synaptic transmission by selectively affecting N- and P/Q-type Ca2+ channels. *J Neurosci.* 2005;25(17):4330-4342.
17. Petrenko AG, Ullrich B, Missler M, Krasnoperov V, Rosahl TW, Sudhof TC. Structure and evolution of Neurexophilin. *Soc Neurosci.* 1996;16(14):4360-4369.
18. Clarris HJ, McKeown S, Key B. Expression of neurexin ligands, the neuroligins and the Neurexophilins, in the developing and adult rodent olfactory bulb. *Int J Dev Biol.* 2002;46(4):649-652.
19. Rodriguez NE, Chang HK, Wilson ME. Novel program of macrophage gene expression induced by phagocytosis of Leishmania chagasi. *Infect Immun.* 2004;72(4):2111-2122.
20. Knight JA, Skol AD, Shinde A, et al. Genome-wide association study to identify novel loci associated with therapy-related myeloid leukemia susceptibility. *Blood.* 2009;113(22):5575-5582.

Downloaded from http://ashpublications.net/blood/article-pdf/118/3/565/1346345/zh802911000565.pdf by guest on 09 June 2024

21. Warnat P, Oberthuer A, Fischer M, et al. Cross-study analysis of gene expression data for intermediate neuroblastoma identifies two biological subtypes. *BMC Cancer.* 2007;7:89.
22. Faria C, Miguens J, Antunes JL, et al. Genetic alterations in a papillary glioneuronal tumor. *J Neurosurg Pediatr.* 2008;1(1):99-102.
23. Song H, Ramus SJ, Kjaer SK, et al. Association between invasive ovarian cancer susceptibility and 11 best candidate SNPs from breast cancer genome-wide association study. *Hum Mol Genet.* 2009;18(12):2297-2304.
24. Cooper S, Broxmeyer HE. Clonogenic methods in vitro for the enumeration of granulocyte-macrophage progenitor cells (CFU-GM) in human bone marrow and mouse bone marrow and spleen. *J Tissue Culture Methods.* 1991;13:77-82.
25. Katsumoto T, Aikawa Y, Iwama A, et al. MOZ is essential for maintenance of hematopoietic stem cells. *Genes Dev.* 2006;20(10):1321-1330.
26. Broxmeyer HE, Orschell CM, Clapp DW, et al. Rapid mobilization of murine and human hematopoietic stem and progenitor cells with AMD3100, a CXCR4 antagonist. *J Exp Med.* 2005;201(8):1307-1318.
27. Mathur AN, Chang HC, Zisoulis DG, et al. T-bet is a critical determinant in the instability of the IL-17-secreting T-helper phenotype. *Blood.* 2006;108(5):1595-1601.
28. Gratzner HG, Leif RC, Ingram DJ, Castro A. The use of antibody specific for bromodeoxyuridine for the immunofluorescent determination of DNA replication in single cells and chromosomes. *Exp Cell Res.* 1975;95(1):88-94.
29. Campbell TB, Basu S, Hangoc G, Tao W, Broxmeyer HE. Overexpression of Rheb2 enhances mouse hematopoietic progenitor cell growth while impairing stem cell repopulation. *Blood.* 2009;114(16):3392-3401.
30. Rhee Y, Allen MR, Condon K, et al. PTH receptor signaling in osteocytes governs periosteal bone formation and intra-cortical remodeling [published online ahead of print December 7, 2010]. *J Bone Miner Res.* doi:10.1002/jbmr.304.
31. Steidl U, Bork S, Schaub S, et al. Primary human CD34+ hematopoietic stem and progenitor cells express functionally active receptors of neuromediators. *Blood.* 2004;104(1):81-88.
32. Lu L, Xiao M, Grigsby S, et al. Comparative effects of suppressive cytokines on isolated single CD34(3+) stem/progenitor cells from human bone marrow and umbilical cord blood plated with and without serum. *Exp. Hematol.* 1993;21(11):1442-1446.
33. Stefansson H, Ophoff RA, Steinberg S, et al. Common variants conferring risk of schizophrenia. *Nature.* 2009;460(7256):744-747.
34. Kim HG, Kishikawa S, Higgins AW, et al. Disruption of neurexin 1 associated with autism spectrum disorder. *Am J Hum Genet.* 2008;82(1):199-207.
35. Broyd SJ, Demanuele C, Debener S, et al. Default-mode brain dysfunction in mental disorders: a systematic review. *Neurosci Biobehav Rev.* 2009;33(3):279-296.
36. Wilke I, Arolt V, Rothermundt M, et al. Investigations of cytokine production in whole blood cultures of paranoid and residual schizophrenic patients. *Eur Arch Psychiatry Clin Neurosci.* 1996;246(5):279-284.
37. Malacarne P, Dallapiccola B. Spontaneous mitoses in direct preparations from peripheral blood of schizophrenic patients. *Experientia.* 1969;25(5):514-515.
38. Muller N, Riedel M, Gruber R, Ackenheil M, Schwarz MJ. The immune system and schizophrenia. An integrative view. *Ann N Y Acad Sci.* 2000;917:456-467.
39. Cohly HH, Panja A. Immunological findings in autism. *Int Rev Neurobiol.* 2005;71:317-341.
40. Enstrom AM, Onore CE, Van de Water JA, Ashwood P. Differential monocyte responses to TLR ligands in children with autism spectrum disorders. *Brain Behav Immun.* 2010;24(1):64-71.
41. Henry MD, Satz JS, Brakebusch C, et al. Distinct roles for dystroglycan, beta 1 integrin and perlecan in cell surface laminin organization. *J Cell Sci.* 2001;114(Pt 6):1137-1144.
42. O'Brien CA, Jia D, Plotkin LI, et al. Glucocorticoids act directly on osteoblasts and osteocytes to induce their apoptosis and reduce bone formation and strength. *Endocrinology.* 2004;145(4):1835-1841.

Downloaded from http://ashpublications.net/blood/article-pdf/118/3/565/1346345/zh802911000565.pdf by guest on 09 June 2024